*Published in: Acta Biomaterialia, (2005), vol. 1, pp. 643-652*
*Status: Postprint (Author's version)*

# Mechanical properties of highly porous PDLLA/Bioglass® composite foams as scaffolds for bone tissue engineering

J.J. Blaker [a], V. Maquet [b], R. Jérôme [b], A.R. Boccaccini [a], S.N. Nazhat [c]

[a] *Department of Materials and Centre for Tissue Engineering and Regenerative Medicine, Imperial College London, London SW7 2BP, UK*
[b] *University of Liège, Centre for Education and Research on Macromolecules Sart-Tilman, B6, B-4000 Liège, Belgium*
[c] *Division of Biomaterials and Tissue Engineering, Eastman Dental Institute, University College London, 256 Gray's Inn Road, London WC1X 8LD, UK*

## Abstract

This study developed highly porous degradable composites as potential scaffolds for bone tissue engineering. These scaffolds consisted of poly-D,L-lactic acid filled with 2 and 15 vol.% of 45S5 Bioglass® particles and were produced via thermally induced solid-liquid phase separation and subsequent solvent sublimation. The scaffolds had a bimodal and anisotropic pore structure, with tubular macro-pores of ~100 µm in diameter, and with interconnected micro-pores of ~10-50 µm in diameter. Quasi-static and thermal dynamic mechanical analysis carried out in compression along with thermogravimetric analysis was used to investigate the effect of Bioglass® on the properties of the foams. Quasi-static compression testing demonstrated mechanical anisotropy concomitant with the direction of the macro-pores. An analytical modelling approach was applied, which demonstrated that the presence of Bioglass® did not significantly alter the porous architecture of these foams and reflected the mechanical anisotropy which was congruent with the scanning electron microscopy investigation. This study found that the Ishai-Cohen and Gibson-Ashby models can be combined to predict the compressive modulus of the composite foams. The modulus and density of these complex foams are related by a power-law function with an exponent between 2 and 3.

**Keywords:** Bioactive glass; Biodegradable composite; Anisotropy; PDLLA; Tissue engineering

## 1. Introduction

The field of tissue engineering has in the last decade offered a new option to supplement existing treatment regimens for the regeneration of bone [1]. One approach has been the implantation of osteoblasts onto three-dimensional (3-D) scaffolds that act as physical supports for these bone cells. However, the structure and properties of 3-D scaffolds are critical in their in vivo performance and there are a number of general key requirements for successful development of scaffolds [2]. The biocompatibility and bioactivity of tissue engineering scaffolds influence the important initial steps related to cell attachment, prior to cell proliferation and differentiation. Ideally, the scaffolds should be porous and the porosity should be both macroscopic for cell growth and migration, as well as microscopic to allow the transport of nutrients and oxygen, as well as the removal of cellular waste products [3]. The scaffolds should also be degradable, thus allowing for eventual tissue in-growth. Furthermore, they should be easily fabricated into 3-D complex shapes in a reproducible and controllable manner. Moreover, the scaffolds should have appropriate and controllable mechanical properties, e.g. elastic constants and compressive strength, thus providing temporary support for cells to enable tissue regeneration [2-5].

One group of materials being considered as scaffolds for bone tissue engineering are porous degradable poly-lactide, polyglycolide or their co-polymers [6,7] with additions of inorganic particles or fibres, such as bioactive glass [8-10] and hydroxy apatite (HA) [11], to impart bioactivity, control degradation kinetics and enhance the mechanical properties. A system currently being developed is based on poly(D,L-lactide) (PDLLA)/Bio-glass®-filled composite foams produced by thermally induced phase separation (TIPS) [12]. Processing of materials using the TIPS method enables the production of foams which exhibit pore anisotropy, which may be controlled to enable the fabrication of scaffolds with tailored porosity appropriate to the tissue concerned [2,13]. Recently, the efficacy of these PDLLA/Bioglass®-filled composites as bone tissue engineering scaffolds has been shown, supporting the migration, adhesion, spreading and viability of MG-63 cells (human osteosarcoma cell line) [14]. Moreover their potential in both bone and lung tissue engineering has been quantitatively demonstrated, using optimal concentrations of 45S5 Bioglass® added to the PDLLA matrix resulting in enhanced cell adhesion and growth in vitro [15].

To date, however, there has been very limited research on understanding the static and dynamic mechanical behaviour of such relatively complex composite foams. In this study, the composites' mechanical response to static and dynamic compression with different volume percentages of Bioglass® particle addition was assessed in the direction of the tubular macro-pores and compared to loading in the transverse direction.

## 2. Experimental

### *2.1. Materials*

Purasorb® PDLLA with a density of 1.26 g $cm^{-3}$ and an inherent viscosity of 1.62 dl/g was obtained from Purac biochem (Goerinchem, The Netherlands) and used without further purification. Dimethylcarbonate (DMC, of >99% purity) was purchased from Sigma Aldrich and used as solvent. Melt-derived 45S5 Bioglass® particles were incorporated as the bioactive phase in the composites. The chemical composition of the glass (in percentage of weight) was as follows: $SiO_2$, 45; CaO, 24.5; $P_2O_5$, 6; $NaO_2$, 24.5. The particle size distribution, specific surface area, porosity and morphological features of this glass have been characterised previously [16], with a finding that the particle size varied between ≈5 and 20 µm with a mean particle size of 4 µm, the density is 2.825 g $c^{-3}$ and surface area is 2.7 $m^2$ $g^{-1}$. The morphology of the 45S5 Bioglass® particles is non-spherical, irregular and angular, as shown in Fig. 1.

***Fig. 1****. SEM micrograph illustrating the irregular and angular morphology of the 45S5 Bioglass® particles.*

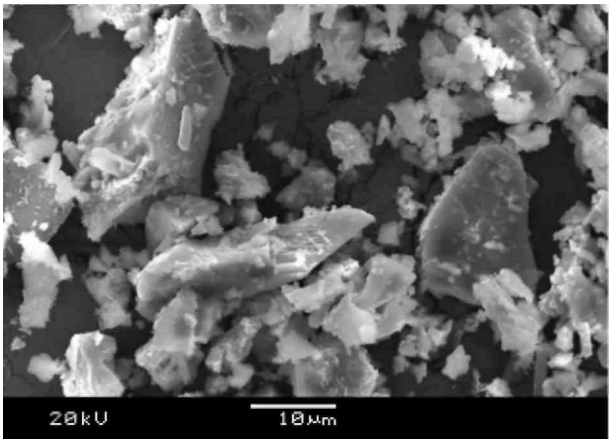


### *2.2. Foam fabrication*

PDLLA and PDLLA/Bioglass®-filled composite foams were prepared by TIPS and subsequent solvent sublimation, which has been described in detail elsewhere [12,13]. Monolithic foams were produced with dimensions of 90 mm diameter and varying in thickness 7-10 mm due to the shape of the vessel base used in fabrication. The following foam systems were investigated: pure PDLLA and composite foams filled with two different amounts of Bioglass® particles, nominally referred to as 2vol.% and 15 vol.% foams. These compositions were chosen based on previous studies conducted on similar composite systems [12,14]. The weight and volume percentages of the Bioglass® phase are given in Table 1.

### *2.3. Methods of analysis*

#### *2.3.1. Scanning electron microscopy*

Scanning electron microscopy (SEM) was used to investigate the anisotropy and homogeneity of the foam microstructure and to assess the porous architecture in different regions within the structure. Foam sections were cut using Wilkinson Sword® razor blades, via continuous downwards slicing to avoid compression damage. Samples were gold coated for 120 s under a current of 20 mA before examination under an accelerating voltage of 20 kV using a JEOL 5610LV SEM (JEOL, USA).

***Table 1** : Foam properties by theoretical calculation of apparent density and porosity*

| Bioglass® content | | Apparent density (P) | % porosity | TGA measured | TGA measured |
|---|---|---|---|---|---|
| wt.% | vol.% | (g $cm^{-3}$) | (*P* from Eq. (1)) | wt.% (at 425 °C) | vol.% (at 425 °C) |
| 0 | 0 | 0.075 ± 0.005 | 94.04 ± 0.40 | - | - |
| 4.76 | 2.18 | 0.077 ± 0.003 | 94.05 ± 0.20 | 4 ± 2 | 1.8 |
| 28.57 | 15.14 | 0.098 ± 0.006 | 93.46 ± 0.40 | 28 ± 6 | 15.6 |

*2.3.2. Overall apparent density*

The volume and mass of foam specimens of ~20 mm in diameter cut from the homogeneous regions of monoliths of the respective foam systems were recorded. Thickness and diameter were measured at six different places for each specimen *(n* — 20 for each foam composition). Using the densities of Bioglass® (2.825 g $cm^{-3}$) and PDLLA (1.26 g $cm^{-3}$) a theoretical porosity was calculated based on the volume percentage of the foam and by comparing its apparent density to the bulk system.

*2.4. Thermal and mechanical analysis*

*2.4.1. Thermogravimetric analysis* Thermogravimetric analyses (TGA) were performed on the composite constituents PDLLA and 45S5 Bioglass® as well as on composite foams using a Stanton Redcroft STA-780 Series Thermal Analyzer. At least three samples for each composite material were analysed and the results averaged to determine the thermal and degradation profiles and residual mass. Scans were performed in an air atmosphere with a temperature range of 35-550 °C at a rate of 20 °C $min^{-1}$. Measurements were taken using a sample mass of 4 ± 0.5 mg for the foams and 10 mg for the Bioglass® powder.

*2.4.2. Quasi-static compressive mechanical analysis* Mechanical compression tests were performed to determine the mechanical properties of the TIPS produced foams. The static stress scan mode of analysis of a Pyris run DMA7e (Perkin-Elmer Instruments, USA) was used. Specimens were cut from the most homogeneous region of the foam to form cubes measuring 5x5x5 $mm^3$. Compression tests were performed axially and transversely, with respect to the direction of the tubular macro-pores using the parallel plate setup. Specimens were tested from 2 kPa to 300 kPa at a rate of 20 kPa $min^{-1}$. The stress and modulus response to strain were recorded. At least five samples of each composition were measured and the results averaged. The modulus (taken at the maximum modulus before the onset of yield point), yield stress (defined as the end of the linear deformation region) and the corresponding strain at yield was also recorded.

*2.4.3. Dynamic mechanical analysis*

Dynamic mechanical analysis (DMA) was carried out on cubic samples (measuring 5x5x5 $mm^3$) obtaine from the homogeneous region of each of the three foam systems. Five repeat specimens were tested in compression under the stress control mode, where a static stress of 30 kPa was initially applied followed by a dynamic stress of 24 kPa. A temperature scan from 25 to 75 °C at a heating rate of 4 °C $min^{-1}$ was applied. Nitrogen was used as purge. The viscoelastic parameters of storage modulus (*E'*), loss modulus *(E")* and mechanical loss tangent (tan *δ)* were recorded as a function of temperature.

**3. Results and discussion**

*3.1. Characterisation of foam pore structure*

Low magnification SEM observations confirmed that no damage was introduced to the foam structures by the chosen cutting technique, using razor blades, confirming previous results [14]. Fig. 2 shows scanning electron micrographs of cross-sections of top, bottom and a stepped side view of the foams produced through TIPS. In general there were four distinct regions observed through the thickness of the foams and these are labelled as regions 1-4. The top of the foam (Region 1) consisted of a skin region of up to 10 µm thickness, which was porous but noticeably denser than the underlying regions. Underneath the top skin layer the foam was more ordered, where the pore anisotropy became apparent (Region 2). This region was less homogeneous than the majority of the foam and was typically 1.5-2.5 mm in thickness. Region 3 within the foams exhibited highly ordered pore architecture, composed of continuous tubular macro-pores of ~100 µm diameter ordered in parallel, and interconnected by micro-pores of ~10-50 µm diameter. This region was typically 5-7 mm in thickness and constituted the majority of the volume of the foam. These homogeneous regions are shown in Fig. 3 for the pure

PDLLA (a) and the PDLLA/ Bioglass® composite foams with Bioglass® inclusion contents of 2 vol.% (b) and 15 vol.% (c), and represent the foam microstructure tested for mechanical properties. The variation in depth of the homogeneous region was due to the shape of the vessel base (slightly convex) used during fabrication. The fourth distinct region was a dense layer on the bottom of the foam, which is analogous to a ladder-like structure that was approximately 30 μm thick (Region 4, in Fig. 2). This region was caused on rapid freezing of the polymer solution; the pore structure was caused by the preferential cooling direction. It is likely that the foam became less ordered with increasing thickness due to effective insulation as the foam cooled down during solvent sublimation. The quality of the foam structure was also determined by the efficiency of the vacuum and solvent collection system, i.e. how often the solvent trap was changed. It has previously been shown that by increasing the polymer to solvent ratio the porous architecture can be controlled, thereby reducing the number of tubular macro-pores and the total porosity [17]. Indeed foams of more isotropic pore structure may be created using the TIPS technique. However in some instances both anisotropic pore architecture and mechanical properties may be beneficial for applications where the structure needs to be made more crush resistant in places, for example in scaffolds of tubular shape for intestinal tissue engineering where collapse of the structure had been observed in vivo [18]. Additionally, by incorporating stiff inorganic glassy or ceramic phases the mechanical properties of the constructs can be tuned; this effect should be more pronounced with more highly anisotropic pore architectures and with scaffolds of lower porosities. The apparent density and porosity of the foams are given in Table 1. Mercury porosimetry was not applied in this investigation to probe the porous structure as this technique is a destructive method for fragile polymer scaffolds, which are prone to simultaneous intrusion and shrinkage under the high pressure of mercury intrusion (up to 2000 bars), as observed in a previous study [17]. The calculated theoretical porosity demonstrated that all the foams exhibited high percentage of porosity (>93%). The addition of 15 vol.% Bioglass® tended to reduce the porosity by ~1% when compared to that of 100% PDLLA and of 2 vol.% PDLLA/Bioglass® foams. This is consistent with previous work where the porosity was also shown to decrease with increasing filler content (up to 40 wt.% Bioglass®) [12]. However, it has been reported that at high filler loadings the pore shapes become increasingly rugose, thereby resulting in a moderately less well-ordered structure [2,12].

***Fig. 2.*** *SEM micrographs of different regions within the foam monolith, demonstrating through-thickness differences of the scaffold architecture. Regions 1-4 are described in the text.*

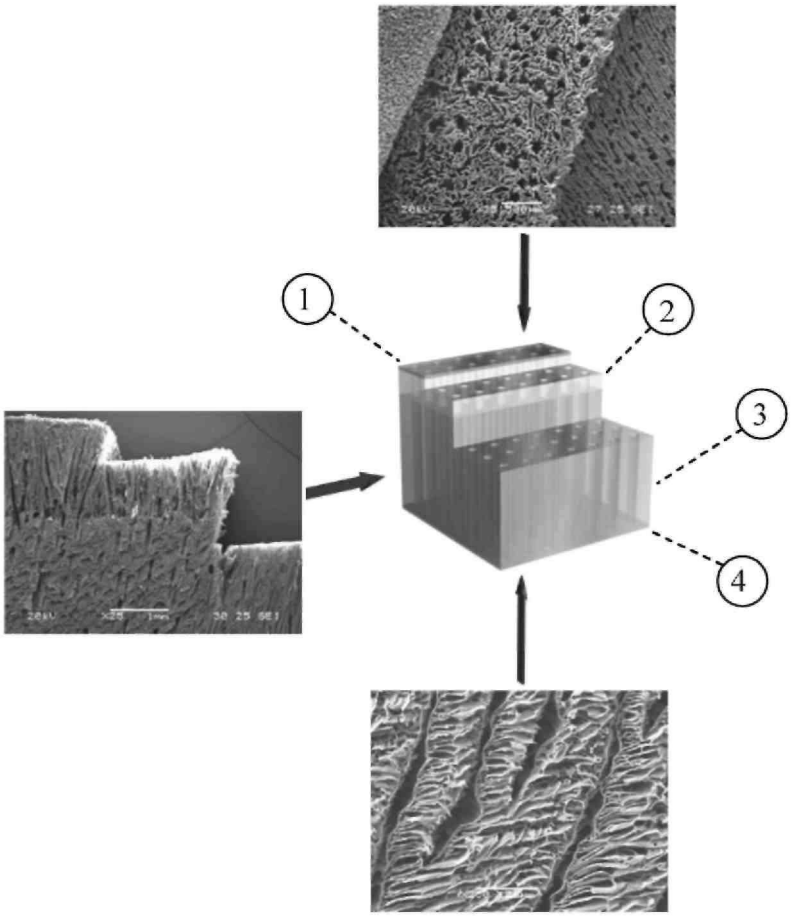

### *3.2. Thermal and mechanical characterisations*

TGA was conducted on the foamed PDLLA, on Bioglass® particles and on the two PDLLA/Bioglass® composite foams. TGA profiles for these materials are shown in Fig. 4. PDLLA foam exhibited no significant change in mass above 425 °C and therefore this temperature was chosen to record the residual mass for all foam systems. It was also shown that below this temperature there are no significant thermal events occurring in the glass, as confirmed in the literature on the thermal treatment of the same Bioglass® [19]. TGA tests conducted on three samples of the composite foams demonstrated that there was slight variability in the amount of Bioglass® present throughout the material, as given in Table 1. Such variation may have been due to partial sedimentation of the Bioglass® particles during foam fabrication.

Fig. 5(a) and (b) shows the compressive stress-strain response of the foams in axial and transverse directions, relative to the tubular macro-pore orientation, respectively. Cubic specimens were cut from the most homogeneous and representative regions of the foams for mechanical analysis, thereby reducing the effect of through-thickness variation in pore architecture. As can be observed, testing in both directions demonstrated mechanical anisotropy in the foams. In the axial direction the compressive stress-strain response agreed well with characteristic behaviours reported in the literature for foam systems [20,21]. This behaviour consisted of three distinct regions: an initial Hookean region in which stress increased in proportion to strain due to compression of the cell elements, a plateau region representing plastic collapse and buckling of the cell elements, and a final region where the stress increased rapidly with strain due to effective densification of the foam structure. Accordingly, the materials showed an increase in modulus in response to strain, which peaked at a certain value and then decreased prior to subsequent strain increase. The plastic collapse region was reduced with increasing Bioglass® content, as shown in Fig. 5(a). The transverse mechanical response to compression shown in Fig. 5(b) displayed a markedly different response to that of the axial response. There appeared to be no obvious micro-failure response due to buckling of the tubular macro-pores, indeed the behaviour of all foams was dominated by the effect of densification of the foams.

***Fig. 3.*** *SEM images of the transversal section showing the typical homogeneous regions of (a) pure PDLLA foam, (b) PDLLA/2 vol.% Bioglass® foam, (c) PDLLA/15 vol.% Bioglass® foam.*

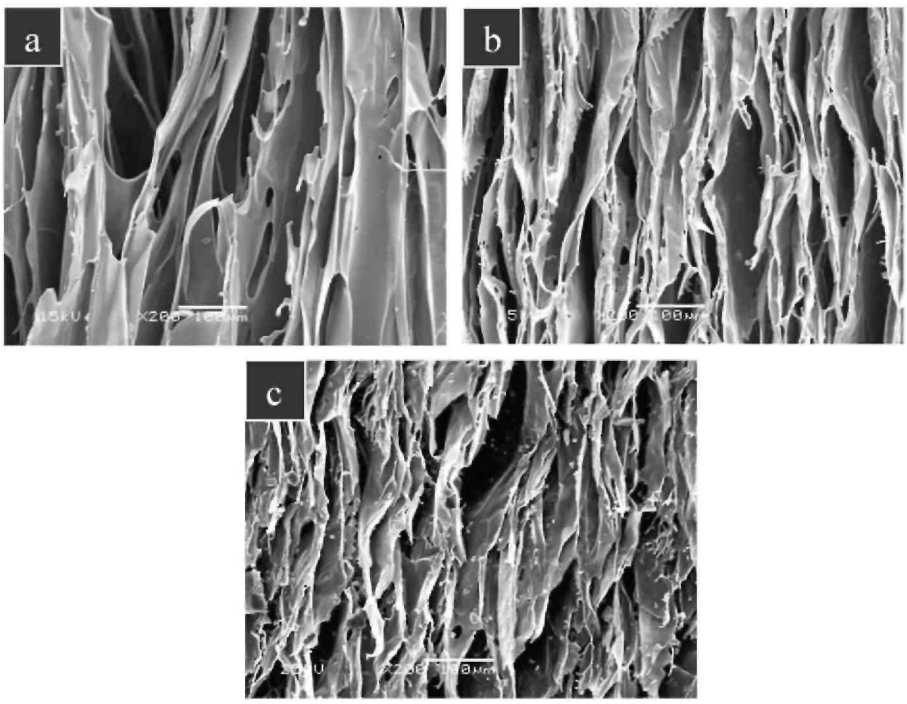

***Fig. 4.*** *TGA of PLA, PLA/Bioglass® and Bioglass® powder.*

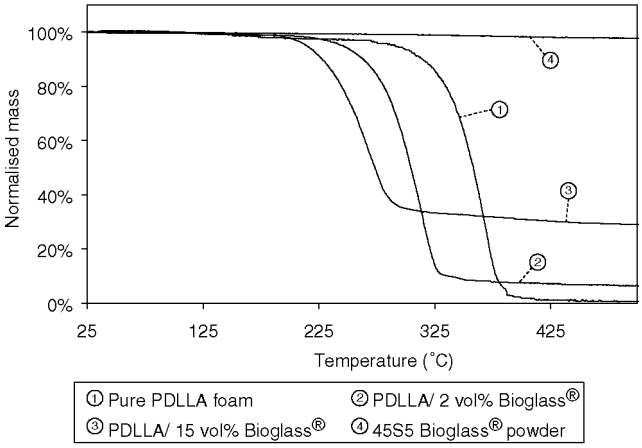


***Fig. 5.*** *(a) Axial stress and modulus response for the various foams. All were tested in the direction parallel to the tubular macro-pores, (b) Transverse stress and modulus response for the various foams. All were tested in the direction perpendicular to the tubular macro-pores.*

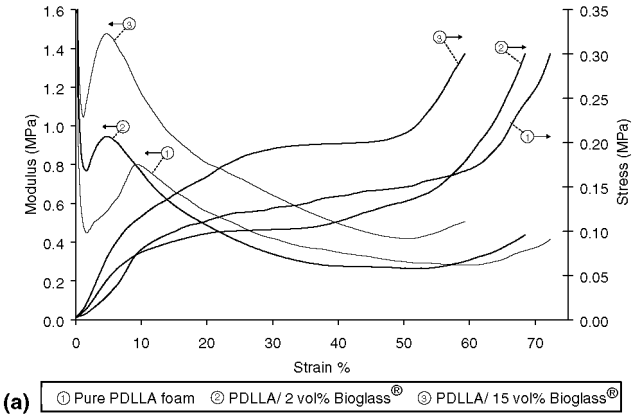


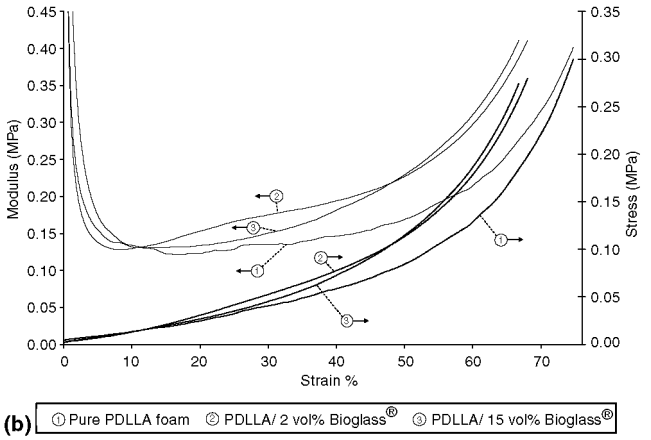


Table 2 summarises the data for the axial compression modulus, yield stress, strain at yield point and the transverse modulus for all the materials. The axial modulus was determined at the maximum modulus, as the stress-strain response varied slightly from sample to sample, due to variation within the foam monolith and the accuracy in cutting the cubic samples. Although there was an increase in the compressive modulus when

comparing the value for the foams with the highest volume percentage of Bioglass®, to that of the PDLLA foams, the results showed no statistical significance differences ($p > 0.05$). This was likely because the porosity is a dominating factor. It seems, therefore, that the 15 vol.% inclusion of Bioglass® particles may not be enough to induce a significant increase of compressive modulus of the foams, as discussed below.

Fig. 6(a) and (b) shows the dynamic mechanical response of the various foams as a function of temperature in terms of storage modulus ($E'$), loss modulus ($E''$), and mechanical loss tangent (tan $\delta$), respectively. There was a trend observed towards an increase in the storage modulus with higher volume fractions of Bioglass®. There was no effect of temperature on the parameters up to the onset of softening above 45 °C, which was defined by an immediate apparent increase in $E$ that may have been due to the immediate densification of the foams as a result of the onset of the PDLLA glass transition. As the temperature increased further there was a significant decrease in $E'$ in all the materials, which was accompanied by peaks in $E''$ and tan $\delta$ that are associated with the glass transition. The broadening of the peak in tan $\delta$ with increasing amounts of Bioglass® is likely to be due to regions of order within the polymer chains in close proximity to the glass particulates. The glass transition temperature ($T_g$), as defined by the temperature where $E''$ reached a maximum, giving $T_g$ values of 56.1 ± 1.2 °C, 55.2 ± 1.4 °C and 56.7 ± 0.8 °C for the PDLLA foams, 2 vol.% and 15 vol.% Bioglass® containing foams, respectively. It can be noted that there was no significant differences ($p > 0.05$) in $T_g$ for the different foam systems.

***Table 2:*** *Quasi-static compression properties of the foams*

| | Axial modulus (MPa) | Axial yield stress (MPa) | Axial yield strain (%) | Transverse modulus (MPa) |
|---|---|---|---|---|
| Pure PDLLA foam | 0.89 ± 0.50 | 0.08 ± 0.03 | 8.2 ± 3.2 | 0.11 ± 0.03 |
| PDLLA/2 vol.% Bioglass® | 0.65 ± 0.40 | 0.07 ± 0.02 | 13.3 ± 7.3 | 0.23 ± 0.10 |
| PDLLA/15 vol.% Bioglass® | 1.20 ± 0.40 | 0.08 ± 0.03 | 7.2 ± 2.4 | 0.16 ± 0.05 |

There were no statistically significant differences ($p > 0.05$) observed between the parameters of the various materials.

### *3.3. Theoretical modelling*

The apparent density ($\rho$) of the scaffolds was determined by using the measured mass and volumes of the foams (Table 1). Porosity ($P$) was calculated using Eq. (1):

$$P = 1 - \frac{\rho}{\rho_0} \qquad (1)$$

where $\rho_0$ is the density of the non-porous material. It has been well documented that the compressive modulus of composite materials increases with increasing filler content and decreases with porosity in highly porous foam systems [8,10,22]. The Gibson and Ashby model given by Eq. (2) has generally been applied to relate the modulus to the density of foams [21]:

$$\frac{E}{E_0} = C\left(\frac{\rho}{\rho_0}\right)^n = C(1-P)^n \qquad (2)$$

where $E$ and $E_0$ are the compressive moduli of the foam and non-porous materials respectively. The constants C and $n$ depend on the microstructure of the foam scaffold. The value of $n$ generally lies in the range $1 < n < 4$ giving a wide range of values for $E/E_0$ at a given density [23]. It has been suggested that for closed-cell porous systems $n$ should have a value in the range of $1 < n < 2$. In their model, Roberts and Garboczi [23] found that if more than 70% of the cell faces are removed, $n$ should increase to 2, indicating that edge bending becomes the dominant mechanism of deformation. For an isotropic open-cell porous structure modelled with pores in cubic arrays this exponent is expected to be 2 [21]. The constant $C$ includes all geometric constants of proportionality needed in the derivation of Eq. (2). Previous experimental data confirm that $C \approx 1$ for foams with dense struts [21]. Several important factors affect the stiffness-porosity relationship, such as whether the pores are open or closed, their geometrical arrangement, in terms of pore orientation and shape, as well as the thickness of the pore walls, and whether the material is periodic or disordered. However, the dependence of $C$ and $n$ on the

microstructure of highly porous materials with more complex pore structures such as the ones investigated in this study is not well understood. The constant C is also dependent on the density of the foam struts.

In this study Eq. (2) was used to investigate the accuracy of the modulus value obtained experimentally for the PDLLA and PDLLA/Bioglass® foams. Firstly, a compressive modulus of non-porous PDLLA ($E_0$) was measured. Samples of dimensions 3x5x6 $mm^3$ were produced by compression moulding at a temperature of 150 °C and a pressure of 2500 psi maintained until the polymer has cooled to room temperature. Compression tests on five repeat samples were performed to BS EN ISO 640 (1997 BS 2782-3: Method 345A:1993. Plastics-Determination of compressive properties). The compressive mechanical properties of the PDLLA used in this investigation are summarised in Table 3. Compression tests revealed that the PDLLA used in this investigation has a compressive modulus ($E_0$) of 1.97 GPa, which is in the range quoted in literature [24].

Using Eq. (2), modulus values for the PDLLA foams of 7 and 0.4 MPa were obtained when using $n$ values of 2 and 3, respectively, and $C = 1$, This suggested that the range $2 < n < 3$ was appropriate to describe the elastic response of the materials in this investigation, especially given that these materials possess interconnected pores.

The value $C = 1$ was chosen based on experimental evidence that this value is the most suitable for foams with dense struts, as presented by Gibson and Ashby [21]. Previously, Hou et al. [25] fabricated high porosity PDLLA foams and found the compressive moduli of scaffolds of 97.2% and 97.7% porosity to be 0.30 MPa and 0.23 MPa, respectively. In another study, Hou et al. [26] related compressive moduli to the porosities of the scaffolds according to the power law relationship (Eq. (2)) and found that $n$ — 2.42 best fit their data. However, in their study, $E_0$ for PDLLA was 296.5 MPa, which appears low.

***Fig. 6.*** *(a) DMA of as-fabricated pure PDLLA foam (1), PDLLA/ 2 vol.% Bioglass® foam (2), PDLLA/15 vol.% Bioglass® (3), showing the storage modulus (E') and loss modulus (E") variation with increasing testing temperature, (b) DMA of as-fabricated pure PDLLA foam (1), PDLLA/2 vol.% Bioglass® foam (2), PDLLA/ 15 vol.% Bioglass® (3), showing the variation of mechanical loss tangent (tan δ) response with increasing temperature.*

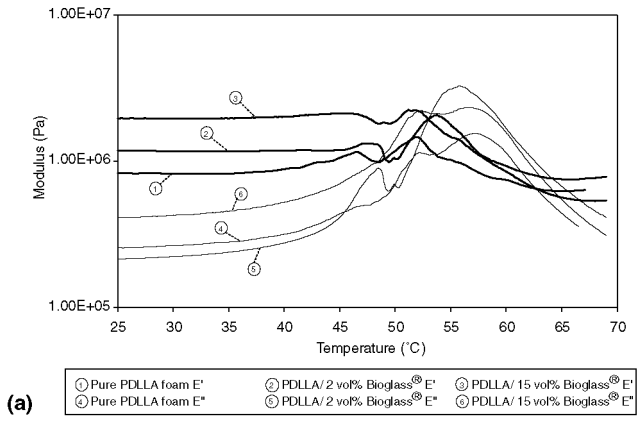


**(a)**

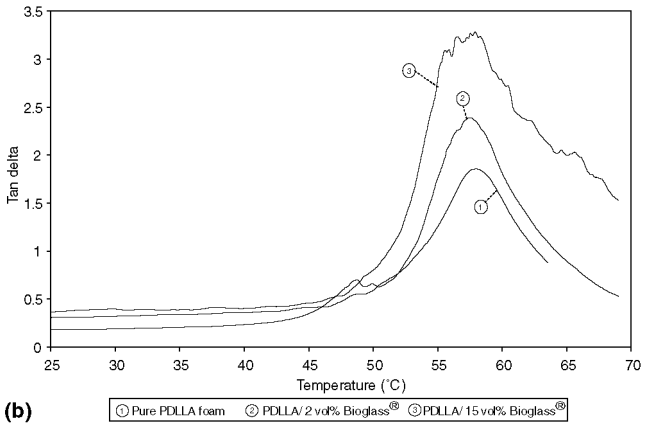


**(b)**

*Published in: Acta Biomaterialia, (2005), vol. 1, pp. 643-652*
*Status: Postprint (Author's version)*

***Table 3** : Compressive mechanical properties of dense PDLLA fabricated by compression moulding*

| Compressive modulus $E_c$ (GPa) | Maximum compressive strength $\sigma_m$ (MPa) | Nominal compressive strain $\varepsilon_{cm}$ (%) at $\sigma_m$ | Compression stress at yield $\sigma_y$ (MPa) | Nominal compressive strain $\varepsilon_{cy}$ (%) at $\sigma_y$ |
|---|---|---|---|---|
| 1.97 ± 0.09 | 86 ± 5 | 5.2 ± 0.4 | 65 ± 5 | 3.4 ± 0.3 |

The effect of incorporating Bioglass® into the PDLLA porous structure and the ability of Eq. (2) to predict the mechanical anisotropy of composite foams was assessed by calculating *n* values based on the experimental data, and maintaining a value $C = 1$, as was known from SEM observations (Fig. 3) that addition of Bioglass® did not substantially change the general structure of the foams. Two approaches were undertaken, firstly; the rule of mixtures (ROM) was used to determine the effective modulus of non-porous composite systems with 2 and 15 vol.% Bioglass®, and the Gibson and Ashby model (Eq. (2)) was applied by using the measured *P* values (given in Table 1) to derive *n* values. The rule of mixtures is defined by Eq. (3):

$$E_c = E_f V_f + E_m V_m \qquad (3)$$

where $E_c$, $E_f$ and $E_m$ are the compressive moduli of the non-porous composite, 45S5 Bioglass® (quoted in the literature as 35 GPa [27]) and PDLLA matrix (measured in this study as 1.97 GPa), respectively, and $V_f$ and $V_m$ are the volume fractions of Bioglass® and PDLLA in the composite foams, respectively. The second approach used the Ishai-Cohen model [22] to quantify the effect of Bioglass® acting as reinforcement within the PDLLA matrix. This equation has been used elsewhere for particulate filled porous foams [10]. The Ishai-Cohen model equation [22] can be written as Eq. (4):

$$E_c = E_m\left(1 + \frac{V_f}{m/(m-1)V_f^{1/3}}\right) \qquad (4)$$

where *m* is the ratio of glass to polymer modulus

$\left(m = \frac{E_f}{E_m}\right)$.

By using Eqs. (3) and (4), the modulus of the porous material is calculated by substituting $E_c$ for $E_0$ in Eq. (2) and the resultant *n* values obtained in this study are shown in Table 4. These values are consistent with the data presented in the literature on the modulus of porous materials [23]. It is clear that the inclusion of Bioglass® particles has only a limited effect on the *n* value, as the calculated *n* value for samples with 0, 2 and 15 vol.% Bioglass® have a coefficient of variation of 2.4% and 4.9% when considering axial and transversal loading, respectively, by using the Ishai-Cohen model for the composite foams. There is a difference however in *n* values between the axial and transverse results, with *n* values being consistently higher for the transverse condition, indicating anisotropy in elastic properties due to the preferred orientation of the tubular macro-pores present in the foams. This suggests that the porosity structure was only slightly affected by the incorporation of Bioglass®, which is in agreement with previous work on similar TIPS produced composite foams [2]. In contrast, the large differences in *n* values found where ROM was used to determine the compressive modulus of the composite scaffolds indicate that the rule of mixtures is not suitable in the present case. The Ishai-Cohen model is suggested for future use in the calculation of elastic modulus of such highly porous foam scaffolds.

The highly porous composite foams developed in this study have potential applications as scaffolds for the engineering of bone, in particular as bone-filling materials for critically sized defects. The bioactivity, degradation behaviour and porous architecture versus mechanical properties of the composites can be tailored thorough composition and by changing the TIPS processing parameters. Bone is anisotropic in nature and its properties depend on the anatomical site and density and on the structural differences between cortical and trabecular bone. The cell size in suspension dictates the minimum pore size required e.g., pore sizes 40-100 μm are necessary for osteoid ingrowth [28]. In regenerating tissues greater than a few millimetres cubic volume a capillary network becomes necessary for gas exchange, provision of nutrients and elimination of waste products for the survival of a large mass of cells. This necessitates the use of optimal bioreactors [29]; depending on the size of the defect the matrix may require seeding with exogenous cells and to be cultured in vitro prior to implantation. There are also trade-offs between mechanical properties and porosity of scaffolds, as opposed to load bearing structures. Highly porous scaffolds may be regarded as temporary mechanical supports for the cells,

possessing sufficient mechanical integrity to support itself in early development and to enable surgical application and manipulation, and resist the forces of wound contraction without damage to the pore structure. Although the pore structure of TIPS produced scaffolds can be tailored to the implant site, their poor mechanical properties make them unsuitable for load bearing applications and additional mechanical support must be provided. Furthermore the results presented in this study represent the mechanical properties of the composites while in the as prepared "dry" state. However, while implanted or in cell culture, it is expected that these properties will change as a consequence of wetting due to the plasticizing effect of water absorbed into the polymers [6]. Therefore further work is being conducted to assess quantitatively the effect of wetting in the short term, as well as the long-term effect of in vitro degradation in simulated body fluid effect on the mechanical, thermal and viscoelastic properties response of these systems

***Table 4** : n Values in Eq. (2) that best fit experimental data, calculated using the rule of mixtures (ROM) or the Ishai-Cohen model [22] approach for the modulus of the investigated foams*

| | Axial compression, *n* values | | Transverse compression, *n* values | |
|---|---|---|---|---|
| Pure PDLLA foam | ROM | Ishai-Cohen | ROM | Ishai-Cohen |
| | 2.73 | 2.74 | 3.48 | 3.48 |
| PDLLA/2 vol.% Bioglass® | 2.96 | 2.87 | 3.33 | 3.24 |
| PDLLA/15 vol.% Bioglass® | 3.19 | 2.83 | 3.92 | 3.56 |

.

## 4. Conclusions

Highly porous PDLLA/Bioglass® composite foams produced by TIPS present anisotropic bi-modal pore architectures with some through thickness variation in pore morphology and density. However the majority of the foam structure is homogenous with continuous tubular macro-pores interconnected by a micro-porous network. There is mechanical anisotropy, which is concomitant with the direction of the tubular macro-pores. At the high porosities of the present foams (>93%) and relatively low volume fractions of Bioglass® (<15 vol.%), there is only a slight trend to stiffening in the composites in comparison with pure PDLLA foams. DMA indicated a glass transition temperature of ~55 °C.

The compressive modulus of the composite foams can be predicted by an approach based on the combination of the Ishai-Cohen and Gibson-Ashby models. The modulus-density relationship of these complex foams is related by a power-law function with exponent between 2 and 3.

## Acknowledgments

The experimental assistance of Miss Shamim Munchie is greatly appreciated. JJB thanks Steven Lamoriniere, Michael Tran (Department of Chemical Engineering), Rebecca Simpson (Department of Mechanical Engineering), and Qizhi Chen (Department of Materials, Imperial College London) for their helpful discussions and assistance with co-extrusion and compression testing. We thank the EPSRC (UK) for funding. CERM is indebted to the "Politique Scientifique Fédérale" in the frame of the "Pôles dAttraction Interuniversitaires (5/03): Chimie et Catalyse Supramolécu-laire", for financial support.

## References

[1] Laurencin CT, Lu HH. Polymer-ceramic composites for bone-tissue engineering. In: Davies JE, editor. Bone engineering. Toronto, Canada: Em Squared Inc.; 2000. p. 462-73.

[2] Boccaccini AR, Maquet V. Bioresourbable and bioactive polymer/Bioglass® composites with tailored pore structure for tissue engineering applications. Compos Sci Technol 2003;63: 2417-2429.

[3] Hutmacher DW. Scaffolds in bone and cartilage. Biomaterials 2000;21:2529-43.

[4] Thomson RC, Shung AK, Yaszemski MJ, Mikos AG. Polymer scaffold processing. In: Lanza RP, Langer R, Vacanti J, editors. Principles of tissue engineering. London: Academic Press; 2000. p. 251-62.

[5] Lu HH, El-Amin SF, Scott KD, Laurencin CT. Three-dimensional bioactive, biodegradable, polymer-bioactive glass composite scaffolds with improved mechanical properties support collagen synthesis and mineralization of human osteoblast-like cells in vitro. J

Biomed Mater Res 2003;64A:465-74.

[6] Wu L, Ding J. In vitro degradation of three-dimensional porous poly(D,L-lactide-co-glycolide) scaffolds for tissue engineering. Biomaterials 2004;25:5821-30.

[7] Lin ASP, Barrows TH, Cartmell SH, Guldberg RE. Microarchitectural and mechanical characterisation of oriented porous polymer scaffolds. Biomaterials 2003;24:481-9.

[8] Zhang K, Ma Y, Francis LF. Porous polymer/bioactive glass composites for soft-to-hard tissue interfaces. J Biomed Mater Res 2002;61:551-63.

[9] Roether JA, Boccaccini AR, Hench LL, Maquet V, Gautier S, Jerome R. Development and in vitro characterisation of novel bioresorbable and bioactive composite materials based on poly-lactide foams and Bioglass® for tissue engineering applications. Biomaterials 2002;23:3871-8.

[10] Zhang K, Wang Y, Hillmyer MA, Francis LF. Processing and properties of porous poly(L-lactide)/bioactive glass composites. Biomaterials 2004;25:2489-500.

[11] Thomson RC, Yaszemski MJ, Powers JM, Mikos AG. Hydroxy-apatite fiber reinforced poly(α-hydroxy ester) foams for bone regeneration. Biomaterials 1998;19:1935-43.

[12] Maquet V, Boccaccini AR, Pravata L, Notingher I, Jerome R. Porous poly(α-hydroxyacid)/Bioglass® composite scaffolds for bone tissue engineering. I. Preparation and in vitro characterisation. Biomaterials 2004;25:4185-94.

[13] Schugens C, Maquet V, Grandfils C, Jerome R, Teyssie P. Biodegradable and macroporous polylactide implants for cell transplantation. 1. Preparation of macroporous polylactide supports by solid-liquid phase separation. Polymer 1996;37:1027-38.

[14] Blaker JJ, Gough JE, Maquet V, Notingher I, Boccaccini AR. In vitro evaluation of novel bioactive composites based on Bio-glass®-filled polylactide foams for bone tissue engineering scaffolds. J Biomed Mater Res 2003;67A:1401-11.

[15] Verrier S, Blaker JJ, Maquet V, Hench LL, Boccaccini AR. PDLLA/Bioglass® composites for soft-tissue and hard-tissue engineering: an in vitro cell biology assessment. Biomaterials 2004;25:3013-21.

[16] Sepulveda P, Jones JR, Hench LL. Characterization of melt-derived 45S5 and sol-gel-derived 58S bioactive glasses. J Biomed Mater Res 2001;58(6):734-40.

[17] Maquet V, Blacher S, Pirard R, Pirard JP, Vyakarnam MN, Jerome R. Preparation of macroporous biodegradable poly(L-lactide-co-epsilon-caprolactone) foams and characterisation by mercury intrusion porosimetry, image analysis, and impedancy spectroscopy. J Biomed Mater Res 2003;66A:199-213.

[18] Blaker JJ, Day RM, Maquet V, Boccaccini AR. Novel bioresorbable poly(lactide-co-glycolide) (PLGA) and PLGA/Bioglass® composite tubular foam scaffolds for tissue engineering applications. Mater Sci Forum 2004; 455-456:415-9.

[19] Clupper DC, Hench LL. Crystallization kinetics of tape cast bioactive glass 45S5. J Non-Cryst Solids 2003;318:43-8.

[20] Hilyard NC. Mechanics of cellular plastics. London: Applied Science; 1982, p. 73-97.

[21] Gibson LJ, Ashby MF. Cellular solids: structure and properties. Oxford: Pergamon Press; 1988, p. 120-68.

[22] Ishai O, Choen LJ. Elastic properties of filled and porous composites. Int J Mech Sci 1967;9:539-416.

[23] Roberts AP, Garboczi EJ. Elastic moduli of model random three-dimensional closed-cell cellular solids. Acta Mater 2001;49: 189-197.

[24] Yang S, Leong K, Du Z, Chua C. The design of scaffolds for use in tissue engineering. Part 1. Traditional factors. Tissue Eng 2001;7:679-89.

[25] Hou Q, Grijpma DW, Feijen J. Preparation of interconnected highly porous polymeric structures by a replication and freeze- drying process. J Biomed Mater Res Part B: Appl Biomater 2003;67B:732-40.

[26] Hou Q, Grijpma DW, Feijen J. Porous polymeric structures for tissue engineering prepared by a coagulation, compression moulding and salt leaching technique. Biomaterials 2003;24:1937-47.

[27] Hench LL. Bioceramics: from concept to clinic. J Am Ceram Soc 1991;74:1487-510.

[28] Whang K, Healy E, Elenz DR, et al. Engineering bone regeneration with bioabsorbable scaffolds with novel macroarchitecture. Tissue Eng 1999;5:35-51.

[29] Shieh SJ, Vacanti JP. State-of-the-art tissue engineering: from tissue engineering to organ building. Surgery 2005; 137( 1): 1-7.